Brain Structure and Function (2019) 224:3321–3338
https://doi.org/10.1007/s00429-019-01967-w

ORIGINAL ARTICLE

Thalamic degeneration in MPTP-treated Parkinsonian monkeys: impact upon glutamatergic innervation of striatal cholinergic interneurons

Rosa M. Villalba[1,3] · Jean-Francois Pare[1,3] · Solah Lee[1,3] · Sol Lee[1,3] · Yoland Smith[1,2,3]

Received: 1 August 2019 / Accepted: 4 October 2019 / Published online: 2 November 2019

Abstract

In both Parkinson's disease (PD) patients and MPTP-treated non-human primates, there is a profound neuronal degeneration of the intralaminar centromedian/parafascicular (CM/Pf) thalamic complex. Although this thalamic pathology has long been established in PD (and other neurodegenerative disorders), the impact of CM/Pf cell loss on the integrity of the thalamostriatal glutamatergic system and its regulatory functions upon striatal neurons remain unknown. In the striatum, cholinergic interneurons (ChIs) are important constituents of the striatal microcircuitry and represent one of the main targets of CM/Pf-striatal projections. Using light and electron microscopy approaches, we have analyzed the potential impact of CM/Pf neuronal loss on the anatomy of the synaptic connections between thalamic terminals (vGluT2-positive) and ChIs neurons in the striatum of parkinsonian monkeys treated chronically with MPTP. The following conclusions can be drawn from our observations: (1) as reported in PD patients, and in our previous monkey study, CM/Pf neurons undergo profound degeneration in monkeys chronically treated with low doses of MPTP. (2) In the caudate (head and body) nucleus of parkinsonian monkeys, there is an increased density of ChIs. (3) Despite the robust loss of CM/Pf neurons, no significant change was found in the density of thalamostriatal (vGluT2-positive) terminals, and in the prevalence of vGluT2-positive terminals in contact with ChIs in parkinsonian monkeys. These findings provide new information about the state of thalamic innervation of the striatum in parkinsonian monkeys with CM/Pf degeneration, and bring up an additional level of intricacy to the consequences of thalamic pathology upon the functional microcircuitry of the thalamostriatal system in parkinsonism. Future studies are needed to assess the importance of CM/Pf neuronal loss, and its potential consequences on the neuroplastic changes induced in the synaptic organization of the thalamostriatal system, in the development of early cognitive impairments in PD.

Keywords Parkinson's disease · Non-human primates · Striatum · vGluT2 · Thalamostriatal · Parafascicular

Introduction

In Parkinson's disease (PD), there is a profound neuronal degeneration of the intralaminar centromedian/parafascicular (CM/Pf) thalamic complex (Henderson et al. 2000a, b; Halliday 2009). We have recently shown that CM/Pf cell loss can also be induced in monkeys treated chronically with low doses of the neurotoxin 1-methyl-4-phenyl-1,2,3,6-tetrahydropyridine (MPTP) (Villalba et al. 2014). In both PD patients and MPTP-treated monkeys, this thalamic neuronal death is an early insult of which the extent is unrelated to the severity of the parkinsonian motor signs (Henderson et al. 2000a, b; Villalba et al. 2014). Despite the fact such thalamic neurodegeneration has long been established in PD (and other neurodegenerative disorders), the impact of CM/Pf cell loss on the integrity of

Electronic supplementary material The online version of this article (https://doi.org/10.1007/s00429-019-01967-w) contains supplementary material, which is available to authorized users.

✉ Rosa M. Villalba
rvillal@emory.edu

[1] Division of Neuropharmacology and Neurological Diseases, Yerkes National Primate Research Center, Emory University, 954, Gatewood Rd NE, Atlanta, GA 303, USA

[2] Department of Neurology, School of Medicine, Emory University, Atlanta, GA, USA

[3] UDALL Center for Excellence for Parkinson's Disease, Emory University, Atlanta, GA, USA

the thalamostriatal glutamatergic system and its regulatory functions upon striatal neurons remains unknown. In the striatum, most neurons are the GABAergic spiny projection neurons (SPNs) that represent over 80% of all striatal neurons in primates (Gerfen et al. 1990; Oorschot 1996; Wickens et al. 2007; Oorschot 2013). The striatum also comprises heterogeneous populations of GABAergic and cholinergic interneurons (ChIs) (Kawaguchi et al. 1995; Bernacer et al. 2007, 2012; Gonzales and Smith 2015). Striatal ChIs have long been recognized as important constituents of the striatal microcircuitry that play key regulatory roles of striatal and basal ganglia function in normal and diseased states (Tepper and Bolam 2004; Bernacer et al. 2007; Lanciego et al. 2012; Tanimura et al. 2018; Zhai et al. 2018; Tanimura et al. 2019; Zheng et al. 2019) Their extensive dendritic and axonal arbors allow them to integrate and transmit information across functionally diverse striatal territories, sub-serving their role in processing attentional salient stimuli in the context of reward-related behaviors (Aosaki et al. 1994; Kimura et al. 2004; Balleine et al. 2007, 2015; Smith et al. 2011; Bradfield et al. 2013; Gonzales and Smith 2015; Bradfield and Balleine 2017; Petryszyn et al. 2018; Peak et al. 2019). One of the main sources of glutamatergic inputs to ChIs is the CM/Pf complex (Lapper and Bolam 1992; Sidibe and Smith 1999; Truong et al. 2009; Galvan and Smith 2011; Bradfield et al. 2013; Smith et al. 2014b; Gonzales and Smith 2015; Matamales et al. 2016; Masilamoni and Smith 2018). In monkeys and rodents, electrophysiological studies have demonstrated that the CM/Pf striatal system is a key regulator of ChI responses to reward-related sensory events and cognitive behaviors related to attention and behavioral switching (Aosaki et al. 1994, 2010; Kimura et al. 2004; Ding et al. 2010; Smith et al. 2011; Bradfield et al. 2013; Balleine et al. 2015; Bradfield and Balleine 2017; Peak et al. 2019).

Thus, knowing the critical role of the CM/Pf complex upon striatal ChIs activity and its importance in mediating complex cognitive behaviors, the goal of the present study is to assess the potential impact of CM/Pf neuronal degeneration on the structural integrity of the thalamostriatal innervation of ChIs in MPTP-treated parkinsonian monkeys.

Some of the results reported here have been published in abstract form (Villalba et al. 2015b; Villalba and Smith 2017).

Materials and methods

Animals

Brain sections from a total six control and six MPTP-treated adult male and female rhesus monkeys (*Macaca mulatta*) raised in the breeding colony of the Yerkes National Primate Research Center were used in this study (Table 1 and Supplementary Table 1). Although six control and six MPTP-treated monkeys were used in this study, each animal was not used in all experiments. The housing, feeding, and experimental conditions used in these studies followed the guidelines by the National Institutes of Health, and are approved by Emory University's Institutional Animal Care and Use Committee (IACUC).

MPTP administration and parkinsonism

Monkeys received systemic injections of MPTP (Sigma-Aldrich, St-Louis, MO) (total dose range 4.3–8 mg/kg, i.m.). During the MPTP treatment, behavioral changes and parkinsonian motor signs were measured with quantitative

Table 1 Control and MPTP-treated monkeys used

	Control			MPTP		
	Monkey	Gender	Age	Monkey	Gender	Age
CM–Pf neurons-stereology	MR 197	Female	13 years, 2 months			
	MR 212	Male	2 years, 7 months	MR 205	Female	14 years, 4 months
	MR 214	Male	10 years, 8 months	MR 245	Female	13 years, 7 months
Striatal ChAT-IR neurons stereology	MR 254	Male	1 years, 9 months	MR 257	Male	6 years, 10 months
	MR 255	Male	3 years, 9 months	MR 258	Male	6 years, 9 months
	MR 256	Male	2 years, 1 months	MR 267	Female	6 years, 11 months
Striatal vGluT2-IR EM analysis	MR 197	Female	13 years, 2 months	MR 183	Female	17 years, 5 months
	MR 212	Male	2 years, 7 months	MR 205	Female	14 years, 4 months
	MR 214	Male	10 years, 8 months	MR 245	Female	13 years, 7 months
Striatal vGluT2-ChAT-IR EM analysis	MR 197	Female	13 years, 2 months	MR 183	Female	17 years, 5 months
	MR 212	Male	2 years, 7 months	MR 205	Female	14 years, 4 months
	MR 214	Male	10 years, 8 months	MR 245	Female	13 years, 7 months

methods that are routinely used in our laboratory (Altar et al. 1986; Singer et al. 1988; Herkenham et al. 1991; Johannessen 1991; Przedborski et al. 2000; Raju et al. 2008; Masilamoni et al. 2010; Villalba and Smith 2011; Mathai et al. 2015; Masilamoni and Smith 2018). Briefly, animals were transferred to an observation cage equipped with eight infrared beams arranged in a square formation on the back and one side of the cage. A computer system was attached and logged the timing of beam crossings (Banner Engineering Corp., Minneapolis, MN). In addition, the animal's spontaneous behavior was also videotaped and a computer-assisted observation method was used to quantify limbs, head, and trunk movements, within a 20-min period. As in our previous studies (Raju et al. 2008; Masilamoni et al. 2010, Villalba and Smith 2011; Mathai et al. 2015; Masilamoni and Smith 2018), the video records were also used to score parkinsonian motor signs with a rating scale similar to that described by Watanabe et al. (2005). This scale assesses key parkinsonian motor signs including gross motor activity, balance, posture, bradykinesia, and hypokinesia.

Animal perfusion and tissue preparation

The monkeys received an overdose of pentobarbital (100 mg/kg; iv) and were then perfused transcardially with cold oxygenated Ringer's solution, followed by fixative containing 4% paraformaldehyde and 0.1% glutaraldehyde in phosphate buffer (PB; 0.1 M, pH 7.4). After perfusion, the brains were removed from the skull, cut into 10–12-mm-thick blocks in the frontal plane and post-fixed in 4% paraformaldehyde for 24–48 h. The blocks of tissue used for electron microscopy studies were stored in cold phosphate-buffered saline (PBS; 0.01 M, pH 7.4) until sectioning into 60-µm-thick coronal sections with a vibrating microtome. Blocks of tissue prepared for light microscopy and stereological studies were immersed in a 30% sucrose solution in PB (0.1 M, pH 7.4) for at least 1 week before being cut into 50-µm-thick coronal serial sections with a freezing microtome. Sections were collected in an anti-freeze solution (1.4% NaH_2PO_4–H_2O, 2.6% Na_2HPO_4–$7H_2O$, 30% ethylene glycol, 30% glycerol dissolved in distilled water) and stored in a − 20 °C freezer until further processing.

Nissl staining

For the analysis of the total number of neurons and the volume of the CM/Pf, a total of nine serial coronal sections (one every fifteenth; 50 µm thick) in three control and three MPTP-treated animals were Nissl stained (see Fig. 1e), and used for unbiased cell counting (see below).

Immunostaining for light and electron microscopy analysis

1. Primary antibodies

All antibodies used in this study are commercially available and have been well characterized using immunoblots on brain tissue or transfected cells, peptide preadsorption, and omission of primary antibodies (Table 2).

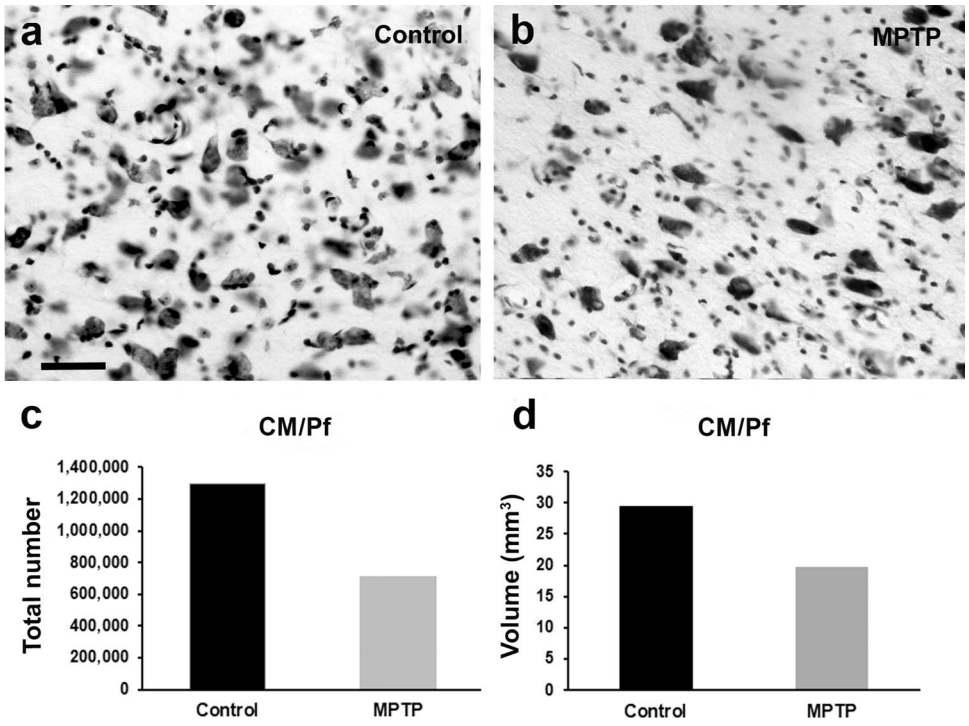

Fig. 1 Cell loss in the intralaminar CM/Pf nuclei of MPTP-treated monkeys. Light microscope images of Nissl–stained coronal sections of the CM in a control (**a**) and a MPTP-treated monkey (**b**). Histograms comparing the total number of neurons (**c**), and the volume of the CM/Pf nuclei (**d**) between control ($N=3$) and MPTP-treated ($N=2$) monkeys. In MPTP-treated parkinsonian monkeys, there is a drastic decrease (45%) in the total neurons number, and in the volume (35%) of the CM/Pf complex compared with controls. Scale bar in **a** (applies to **b**) = 50 µm

Table 2 Antibody information

Antigen	Immunogen	Species	Vendor	References
Calbindin-D-28-K	BALB/c mice immunized with a purified bovine kidney calbindin-D-28K	Mouse	Sigma, Catalog No C9848	Masilamoni et al. (2011), Villalba et al. (2014)
Choline acetyltransferase (ChAT)	Native choline acetyltransferase purified from human placenta	Goat	ProSci Inc. (Poway, CA) Catalog No 50-265	Gonzales and Smith (2015), Masilamoni and Smith (2018), Yalcin-Cakmakli et al. (2018), Lallani et al. (2019)
Vesicular glutamate 2 transporter (vGluT2)	COOH terminus human vGluT2-aa 560-578	Rabbit	Mab Technologies (Atlanta, GA), Catalog No VGT2-6	Raju et al. (2008), Villalba and Smith (2010, 2011, 2013, 2018)

- *Calbindin-D-28k (Cb) antibody*. A monoclonal anti-Calbindin-D-28K (mouse IgG1 isotype) antibody was used to recognize specifically Cb in brain tissue. The pattern of thalamic labeling was like that described in previous non-human primate studies using the same or different Cb antibody (Masilamoni et al. 2011; Villalba et al. 2014).
- *Choline acetyl transferase (ChAT) antibody*. A polyclonal ChAT antibody raised in goat was used. The overall pattern of immunostaining obtained with this antiserum was confined to brain areas known to express detectable levels of ChAT and that preadsorption immunoshistochemical assays resulted in the reduction of ChAT staining in these regions (see Gonzales and Smith 2015, Masilamoni and Smith 2018). Western blot analysis from human brain of placental tissue showed a distinct band at 68 kDa that corresponds to the molecular weight of enzymatically active ChAT (Masilamoni and Smith 2018).
- *vGluT2 antibody*. A rabbit anti-human vGluT2 polyclonal antibody (Mab Technologies) was used. This antiserum was obtained from rabbits (Covance, Princeton, NJ) immunized against a peptide corresponding to amino acids 560–578 of the COOH terminus of the human vGluT2 (hvGluT2). The specificity of vGluT2 antibody on monkey tissue was determined by Western immunoblots and light microscopy preadsorption immunohistochemical analyses, as previously described (Raju et al. 2008).

2. Light microscopy (LM): ChAT-immunostaining in the striatum and Cb-immunostaining in the CM/Pf nuclei

Serial striatal sections and sections containing the CM/Pf nuclei from control and MPTP-treated parkinsonian monkeys were treated at room temperature (RT) with sodium borohydride (1% in PBS) under the hood (20 min), rinsed in PBS (4–5 times), followed by a pre-incubation in a solution containing 1% Normal Horse Serum (NHS), 0.3% Triton-X-100, and 1% bovine serum albumin (BSA) in PBS. Sections were then incubated for 24 h at RT in a PBS solution (with 1% NHS, 0.3% Triton-X-100, and 1% BSA) containing the primary antibody. A goat anti-ChAT (dilution: 1:100) antibody was used for striatal sections, and a mouse anti-Cb antibody (dilution 1:4000) for thalamic immunostaining. Following the primary antibody incubations, the sections were thoroughly rinsed in PBS and incubated for 90 min at RT with their respective secondary antibodies (biotinylated horse anti-goat IgGs for ChAT; biotinylated horse anti-mouse IgGs for Cb; Vector, Burlingame, CA) diluted at 1:200 in a PBS solution containing 1% normal non-immune serum, 0.3% Triton-X-100, and 1% BSA. This was followed by washes in PBS and a 90-min incubation at RT in the avidin–biotinylated peroxidase complex (ABC; Vector, Burlingame, CA) diluted at 1:100 in the same diluents as for the primary and secondary antibodies. Finally, sections were rinsed in PBS and TRIS buffer (0.05 M, pH 7.6) before being placed in a solution containing 0.025% Diaminobenzidine (3,3′-diaminobenzidine tetrahydrochloride, DAB; Sigma, St Louis, MO), 0.01 M imidazole (Fisher Scientific, Norcross, GA), and 0.005% H_2O_2 for 10 min at RT. The reaction was stopped by washes in PBS, and the sections were mounted on gelatin-coated slides, dehydrated in alcohol, immersed in toluene and coverslipped with Permount. Finally, the tissue was examined with a Leica DMRB light microscope (Leica Microsystems, Inc., Bannockburn, IL) and images were taken with a CCD camera (Leica DC 500; Leica IM50 software). For low magnification images, slides were scanned using a ScanScope CS scanning system (Aperio Technologies, Vista, CA). Digital representations of the slides were saved and analyzed using ImageScope software (Aperio Technologies).

3. Electron microscopy (EM)

Single pre-embedding immunoperoxidase for vGluT2. In this study, vGluT2 staining was used as a marker for glutamatergic thalamostriatal projections (Fremeau et al. 2001; Raju et al. 2008; Villalba and Smith 2010, 2011, 2013, 2018; Smith et al. 2014a). Sections were treated with a 1% sodium borohydride solution, placed in a cryoprotectant solution (PB 0.05 M; pH 7.4; 25% sucrose, and 10% glycerol), frozen

at − 80 °C for 20 min, thawed, and returned to a graded series of cryoprotectant solution diluted in PBS. They were then washed in PBS and pre-incubated for 1 h at RT in a solution containing PBS, 1% normal goat serum (NGS), and 1% bovine serum albumin (BSA), then incubated in the primary rabbit anti-vGluT2 antibody (dilution 1:5000) for 48 h at 4 °C, and their localization was revealed using the avidin–biotin–peroxidase complex method (ABC-Vectastain Standard kit, Vector Labs) with a DAB solution used as chromogen for the peroxidase reaction, as described above and in our previous studies (Raju et al. 2008; Villalba and Smith 2010, 2011, 2013, 2018; Villalba et al. 2015a). Immunostained striatal sections were post-fixed in osmium tetroxide, dehydrated in alcohol and propylene oxide, embedded in resin (Durcupan, ACM, Fluka) for at least 12 h, mounted on slides and coverslipped. The resin was polymerized at 60 °C for 48 h (see Villalba et al. 2016).

Double immunolabeling for vGluT2 and ChAT. Striatal sections were incubated overnight at RT with a cocktail of rabbit vGluT2 antibody (dilution 1:5000) and a goat anti-ChAT antibody (dilution 1:100). All antibodies were diluted in Tris-buffered saline (TBS)-gelatin buffer (0.02 M Tris, 0.15 M NaCl, 1 µl/ml fish gelatin, pH 7.6) with 1% nonfat dry milk to block the nonspecific sites. After rinses with TBS-gelatin, the sections were incubated with goat-anti-rabbit IgGs conjugated with 1.4-nm gold particles (dilution 1:100; Nanoprobes Inc.), then rinsed with TBS-gelatin and transferred to a 1% aqueous sodium acetate solution before the intensification of the gold particles with HQ silver kit (Nanoprobes Inc.). After silver intensification, sections were incubated in biotinylated horse anti-goat antibodies (dilution 1:200; Vectastain Standard kit, Vector Labs), and processed with ABC and DAB, as described for the single pre-embedding peroxidase immunolabeling localization of ChAT, except that Triton-X-100 was omitted from the diluent solutions.

Ultrathin sectioning and EM analysis. Blocks of immunostained tissue (from caudate or putamen nuclei) were removed from the slides, and glued on top of resin blocks, trimmed and cut into 60-nm ultrathin serial sections with an ultramicrotome (Ultracut T2; Leica, Germany), and collected on single-slot Pioloform-coated copper grids. Ultrathin sections were then stained with lead citrate for 5 min and examined with a JEOL/JEM-1011 electron microscope (see Villalba et al. 2016). Electron micrographs were taken and saved at 40,000 × magnification with a CCD camera (Gatan Model 785-DigitalMicrograph software, version 3.10.1; Gatan, Inc., CA).

Control experiments. In a series of control experiments, sections were processed as described above, but without primary antibodies (as a control for the specificity of secondary antibodies). The control sections for single labeling experiments were completely devoid of immunostaining. In case of controls for the double labeling experiments, each antibody was omitted in turn from the incubation solutions, while the rest of the procedure was unchanged. In these sections, there was a complete lack of immunostaining for the omitted antibody, but no effect on the pattern and intensity of immunostaining associated with the other primary antibody.

Unbiased stereology and volume analysis

The total number of ChIs and CM/Pf neurons was estimated using the unbiased stereological method of the optical fractionator (Gundersen and Osterby 1981; Gundersen 1986; West 1999; Schmitz and Hof 2005), and the Cavalieri's principle was used to estimate the volume (StereoInvestigator, MicroBrightField, Inc.). Stereological cell count and volume analyses were performed using serial coronal sections (sectioned thickness, 50 µm). Because of tissue shrinkage, the final mounted mean section thickness was estimated under the microscope from at least six measurements/section obtained by moving the focus from the top to the bottom surface of the tissue with the *Z*-axis position encoder of the stereology system. Then, the numerical density (number of neurons/mm^3) for each ROIs was calculated. The precision of the estimates of the total number of neurons (n), and the volume was evaluated by the coefficient of error (CE).

Total number of neurons and volume estimation of the Intralaminar (CM/Pf) nuclei. Every fifteenth serially collected coronal sections through the full rostrocaudal extent of CM/Pf (9 sections per animal) were Nissl-stained and used for unbiased neurons counting and volume Cavalieri's analysis. Adjacent Cb-immunostained sections were used to help delineate the borders of the CM/Pf complex (see Villalba et al. 2014). The ROIs were delineated using a low magnification objective, and a 100 × oil-immersion (NA: 0.7) was used for neuronal counting. The grid spacing was 600 × 600 µm^2 and the dissector area was 75 × 75 µm^2 with a height of 24 µm (guard zone of 3 µm). For the Cavalieri's analysis of the CM/Pf complex volume, the same number of sections and ROIs were used, and the distance between points was 600 × 600 µm^2. With these parameters, we obtained a CE (Gundersen, $m = 1$) between 0.03 and 0.05 for the estimation of the total number of CM/Pf neurons, and 0.03 for the estimation of the total volume of CM/Pf complex (Gundersen, $m = 1$).

Total number of cholinergic interneurons (*ChI; ChAT-IR) and volume estimation of the striatum*. The delineation of the regions of interest (ROIs), namely the caudate nucleus (head and body) and putamen (pre- and post-commissural), was performed at low magnification, while the count of ChAT-IR neurons (profiles) was done using a 40 × oil-immersion objective (numeric aperture, NA: 0.7). In our analysis, the individual array elements in the virtual grid were separated by 1500 × 1500 µm^2, and the dissectors had an area of

800 × 800 µm^2 with a height of 24 µm, and a guard zone of 3 µm (see Villalba et al. 2014). The total number of sections used per animal (between 15 and 17), the fraction of sections (1 every 24 for 5 animals, and 1 every 30 for 1 animal), the counting frame/dissector size, (Henderson et al. 2000b) and the dimensions of the virtual grid placed over the ROIs let us to obtain a CE (Gundersen, $m=1$) between 0.03 and 0.06 (Gundersen 1986; Glaser and Wilson 1998). For the estimation of the striatal volume, we used the Cavalieri's method, and the point-counting technique (for stereological cross-sectional area estimation) with a distance between points of 400 × 400 µm^2 on the same ROIs, and number of sections that were used for the neuronal (ChAT-IR) counting (CE between 0.01 and 0.03).

Statistical analysis

Inter-individual difference between animals of the same group was tested using one-way ANOVA. Stereological results (for striatal ChI) and the results for the density of striatal vGluT2-terminals were expressed as mean ± SEM and compared using Student's *t* test. The results about the relative prevalence of glutamatergic inputs (vGluT2-positive) to striatal ChIs were expressed as proportions of vGluT terminals in contact with ChAT-positive profiles, and the differences between control and MPTP-treated monkeys were statistically assessed using Chi-square analysis. Statistical differences were determined using Sigmaplot 14.0 sofware.

Photomicrographs production

Light and electron microscopic micrographs shown in this manuscript were digitally acquired, imported in TIFF format to Adobe Photoshop (CC 2019; Adobe Systems, San Jose, CA) and adjusted only for brightness and contrast, to optimize the quality of the images for analysis. Micrographs were then compiled into figures using Adobe Illustrator CS6.

Results

Total number of neurons and volume of the CM/Pf nuclei in control and MPTP-treated parkinsonian monkeys

This first series of experiments was achieved to confirm our previous observations (Villalba et al. 2014) that the chronically MPTP-treated monkeys used in the present study underwent severe neuronal degeneration of the CM/Pf complex. The results of this unbiased quantitative analysis showed that the total number of Nissl-stained neurons in the CM/Pf nuclei of MPTP-treated monkeys ($n=708{,}800$; CE = 0.05) was 45% lower than that in control animals ($n=1{,}295{,}645$; CE = 0.03) (Fig. 1c, e). In line with these observations, the Cavalieri's analysis revealed a 35% volume reduction of the CM/Pf nuclei in the MPTP-treated monkeys (20 mm^3; CE = 0.03) compared with controls (29 mm^3; CE = 0.03) (Fig. 1d, e). These observations provide further evidence that CM/Pf complex is pathologically affected in parkinsonian monkeys, as reported in PD patients (Henderson et al. 2000a, b; Halliday et al. 2005; Brooks and Halliday 2009; Halliday 2009).

Total number and density of striatal cholinergic interneurons (ChI) in control and MPTP-treated parkinsonian monkeys

To assess potential changes in the cellular substrate that could mediate CM/Pf interactions with ChIs in control and parkinsonian monkeys, we determined if the total number of ChIs was altered in various striatal regions of MPTP-treated monkeys compared with controls. In both groups, ChIs were immunostained with a ChAT antibody (Table 2). At the light microscopic level, there was no obvious difference in the overall pattern of ChAT staining and the morphology of ChAT-positive neurons in the caudate nucleus and putamen of control vs parkinsonian monkeys (Fig. 2a, b). In both groups of animals, the length and ramification of the immunostained dendritic tree of individual neurons were consistent with previously reported data (Mesulam et al. 1984; DiFiglia 1987; Yelnik et al. 1993; Schafer et al. 1995; Gonzales et al. 2013; Gonzales and Smith 2015). In general, thick aspiny primary dendrites branched close to the large, polygonal, ovoidal or fusiform cell bodies, and gave rise to a profuse dendritic arbor that often extended over long distances within the striatal neuropil (Fig. 2c–f).

The total number of ChAT-IR neurons and the volume of the caudate nucleus and putamen were estimated in three control and three parkinsonian monkeys using an unbiased stereological approach (see Table 1). Overall, there was no statistically significant difference (*t* test) in the total number of ChIs in various regions of the caudate nucleus and putamen between control and parkinsonian monkeys, albeit a trend towards an increased number of ChIs in the head of the caudate nucleus of MPTP-treated monkeys (Fig. 3a). Similarly, despite modest average decreases (13–24%) in the volume of the caudate nucleus and putamen of parkinsonian monkeys, these differences were not statistically significant (*t* test) (Fig. 3b). However, when the density of ChAT-IR neurons was compared across striatal regions, a significant increase (*, statistically significant, *t* test) of 40% and 27% was found in the head (*t* test, $P=0.043$) and body (*t* test, $P=0.045$) of the caudate nucleus of MPTP-treated monkeys, respectively (Fig. 3c).

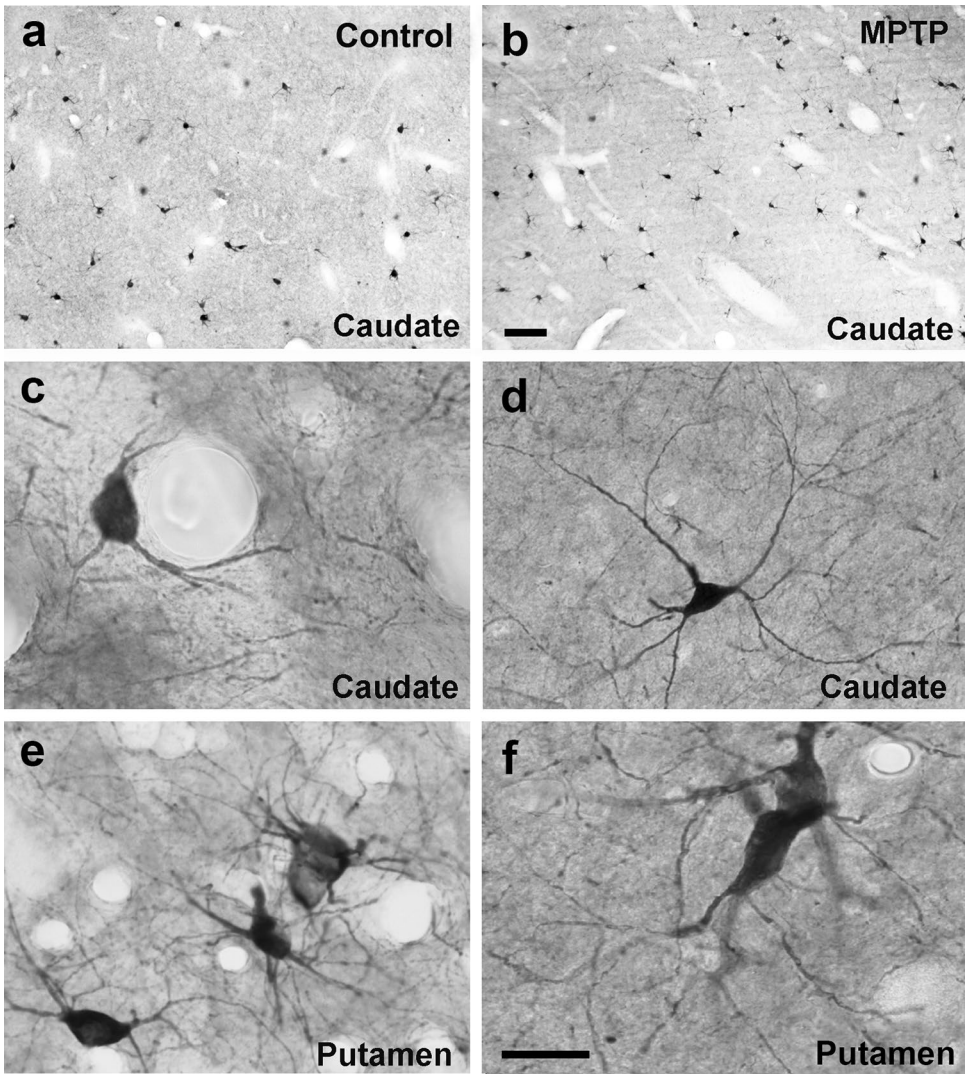

Fig. 2 Light micrographs of striatal cholinergic interneurons in the caudate (**a**–**d**) and putamen (**e**, **f**) of control (**a**, **c**, **e**) and MPTP-treated monkeys (**b**, **d**, **f**). In both control and parkinsonian monkeys, these neurons have large cell bodies with different morphologies (ovoid, elongated or triangular) and prominent primary dendrites. The length and ramification of their immunostained dendritic trees vary, but usually the thick primary dendrites branch close to the cell body and give rise to dendritic trees that often extend over long distances in the striatal neuropil. Scale bar in **b** (applies to **a**) = 200 µm and in **f** (applies to **c**–**e**) = 25 µm

Density of thalamostriatal (vGluT2-positive) axo-spinous and axo-dendritic synapses in control vs MPTP-treated parkinsonian monkeys

In this series of experiments, we determined whether the density of vGluT2-positive thalamostriatal terminals was altered in various striatal regions of parkinsonian monkeys. Thus, striatal tissue from three control and three parkinsonian monkeys was immunostained for vGluT2 using the immunoperoxidase method. From these sections, blocks of tissue were dissected out from different striatal regions (head and body of caudate nucleus, pre- and post-commissural putamen), cut in ultrathin sections and scanned in the electron microscope. At the electron microscopy level, vGluT2-positive terminals were identified by the presence of the amorphous electron-dense peroxidase deposit (Fig. 4). The ultrastructural features of these boutons were consistent with those described in previous studies from our group and others (Lacey et al. 2005; Raju et al. 2006, 2008; Villalba and Smith 2010, 2011, 2013, 2018; Deng et al. 2013; Zheng et al. 2019). To quantify the density of vGluT2-positive boutons, 50 random images per striatal region/animal were taken (a total of 150 pictures per striatal region) at 40,000 × magnification from the most superficial sections of the block to ensure optimal vGluT2 antibody penetration. From these images, the number of vGluT2-positive terminals that formed clear synapses was counted, and their postsynaptic targets were categorized as spines or dendrites. As shown in Fig. 5, two main conclusions can be drawn from this analysis: (1) the relative density of vGluT2-positive terminals is homogeneous across the various striatal regions, ranging from ~ 4 to 7×10^3 vGluT2-containing terminals/mm^2 of striatal tissue and (2) There is no significant difference in the density of vGluT2-positive terminals in all striatal regions between control and MPTP-treated parkinsonian monkeys (Fig. 5).

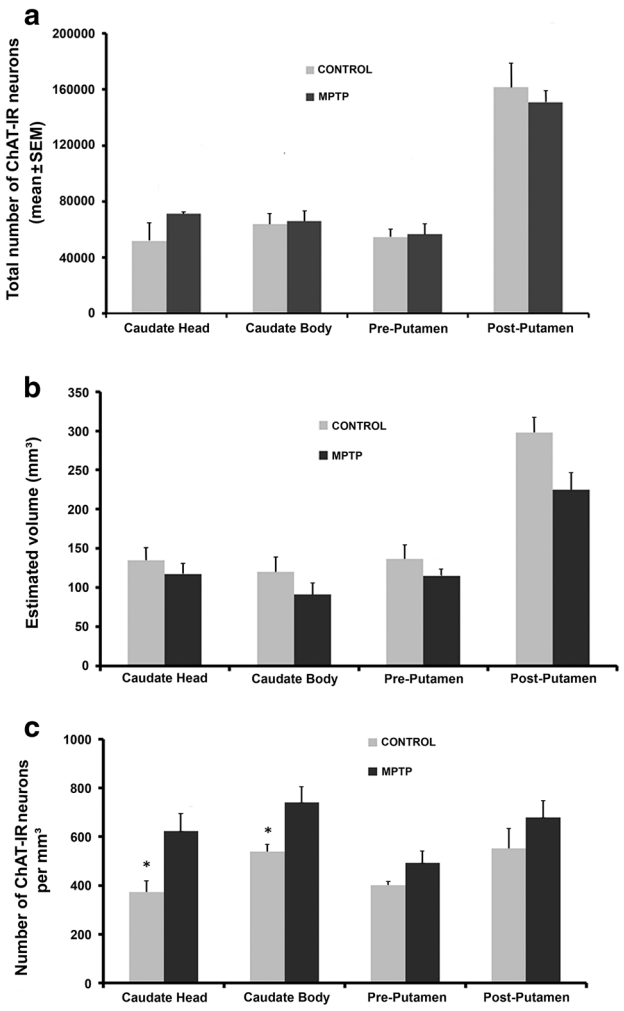

Fig. 3 Stereological analysis of the number and density of cholinergic interneurons (ChAT-IR neurons) in the striatum of control and MPTP-treated parkinsonian monkeys. **a** Histograms comparing the change in the estimated total number (mean ± SEM) of ChAT-IR neurons in the head and body of the caudate nucleus, and in the pre- and post-commissural putamen of control ($N=3$) and MPTP-treated parkinsonian monkeys ($N=3$). **b** Stereological estimated volume (Cavalieri's analysis) of the caudate nucleus and putamen in control ($N=3$) and MPTP-treated ($N=3$) monkeys. The values in the histograms represent the mean ± SEM per group. **c** Density of ChAT-IR neurons in the caudate nucleus and putamen of control ($N=3$) and MPTP-treated parkinsonian ($N=3$) monkeys. Note the increased density of cholinergic interneurons in the head and body of the caudate nucleus (*, *t* test; head, $P=0.043$ and body, $P=0.045$)

Thalamostriatal glutamatergic inputs (vGluT2-positive) onto striatal ChAT-positive dendrites in control vs MPTP-treated parkinsonian monkeys

The goal of this series of experiments was to determine if the proportion of ChAT-positive dendrites contacted by vGluT2-positive thalamostriatal terminals differs between control and parkinsonian monkeys. To address this issue, we used a double pre-embedding immunolabeling approach to identify ChAT-positive dendrites with immunoperoxidase and vGluT2-positive terminals with silver-intensified gold particles in the same striatal tissue. Thus, in the electron microscope, ChAT-immunopositive dendrites were identified by the electron-dense DAB reaction product, whereas vGluT2-positive terminals were localized by the presence of silver/gold particles (Fig. 6). A terminal was categorized as vGluT2-positive if it contained two or more gold particles (Fig. 6a, b, e). As depicted in Fig. 6, both sets of labeled elements were easily distinguishable from each other, and commonly overlapped in the striatum (Fig. 6).

Thus, double immunostained sections of caudate nucleus and putamen in three control and three parkinsonian monkeys were used in these experiments. In the electron microscope, quantitative data were collected exclusively from the most superficial sections of tissue blocks to ensure optimal penetration of both antibodies (Fig. 6). From regions of the caudate nucleus and putamen that were co-labeled for vGluT2 and ChAT, 90 micrographs of ChAT-positive dendrites (30 dendrites/monkey) in the close vicinity of gold-labeled vGluT2-containing terminals were taken in the caudate nucleus and putamen. For each ChAT-positive dendrite, we determined if it formed asymmetric synapses with vGluT2-positive and/or vGluT2-negative terminals. In both, the caudate nucleus and putamen of control and MPTP-treated animals, over 80% of the ChAT-positive dendrites formed asymmetric synapses with vGluT2-negative terminals. As shown in Fig. 7, ~ 10% ChAT-positive dendrites examined formed asymmetric synapses with vGluT2-positive terminals in the caudate nucleus of both control and parkinsonian monkeys, while this percentage increased from ~ 14 to ~ 20% in the putamen of these animals. The statistical analysis (Chi-square test) showed no significant difference in the proportion of ChAT-positive dendrites that formed asymmetric synapses with vGluT2-positive terminals between control and parkinsonian monkeys (Fig. 7).

Discussion

Despite clear evidence that CM/Pf neurons undergo profound degeneration in PD (Henderson et al. 2000a, b; Halliday et al. 2005; Brooks and Halliday 2009; Halliday 2009) and that thalamic inputs from CM/Pf are key regulators of striatal ChIs activity (Akins et al. 1990; Meredith and Wouterlood 1990; Lapper and Bolam 1992; Sidibe and Smith 1999; Brown et al. 2010; Ding et al. 2010; Galvan and Smith 2011), this study is the first assessment of the potential impact of CM/Pf neuronal loss on the anatomy of the synaptic connections between thalamic terminals and ChIs in an animal model of parkinsonism. The following

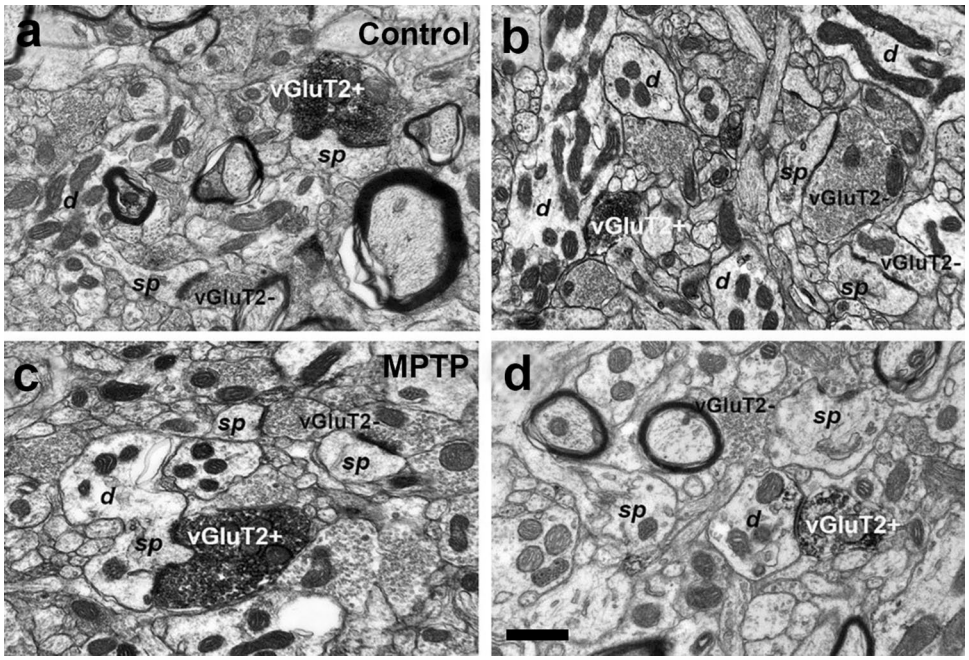

Fig. 4 Electron micrographs of vGluT2-positive (vGluT2+) terminals forming asymmetric synapses with dendrites (**d**) and dendritic spines (sp) in the caudate (**b**, **c**) and putamen (**a**, **d**) of control (**a**, **b**) and MPTP-treated-parkinsonian monkeys (**c**, **d**). In the same field, vGluT2-negative (vGluT2-) terminals form asymmetric synapses with dendritic spines. Scale bar in **a** (applies to **b** and **c**) and in **d** = 0.5 μm

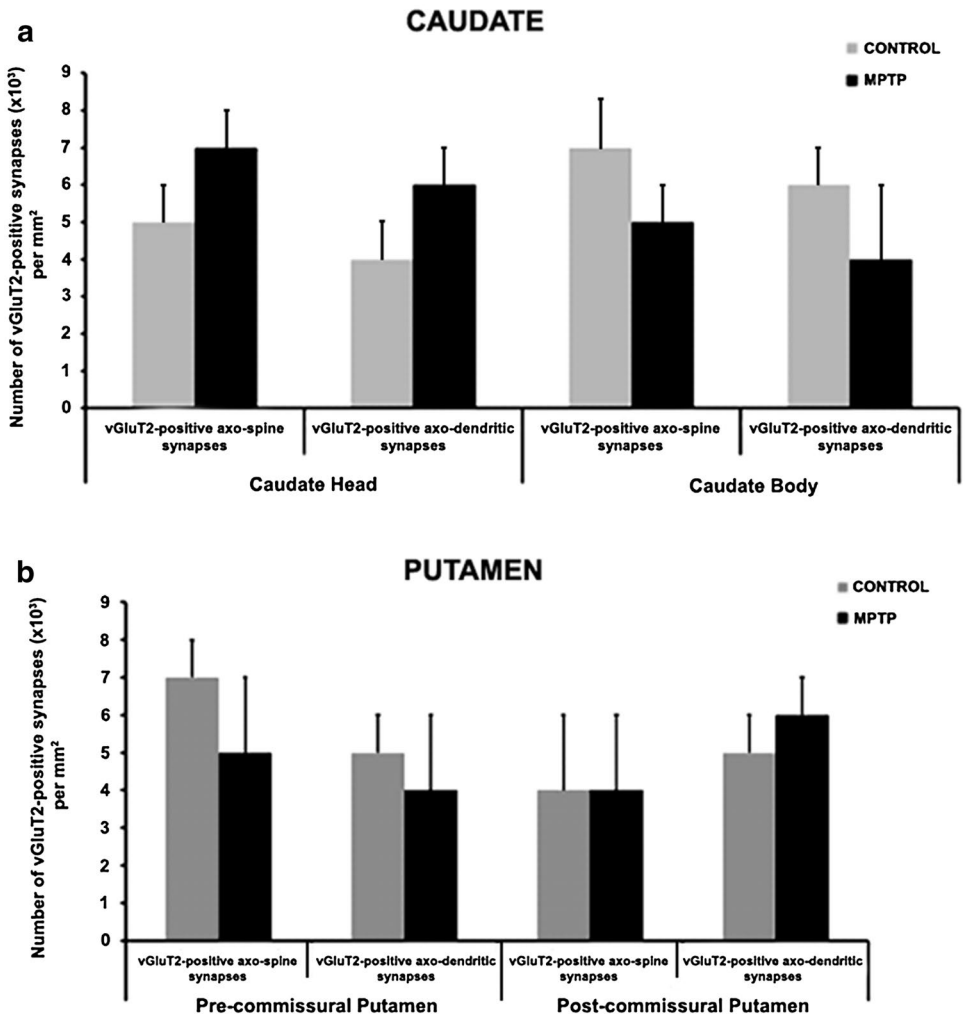

Fig. 5 Histograms comparing the density of vGluT2-positive terminals in the caudate (**a**) and putamen (**b**) of control ($N = 3$) and MPTP-treated ($N = 3$) parkinsonian monkeys. This analysis revealed that the density of vGluT2 + terminals forming synapses onto dendrites and spines in both the head and body of the caudate, and the pre- and post-commissural putamen was not statistically different between control and MPTP-treated monkeys (*t* test, *P* values: Caudate head axo-spine = 0.442; axo-dendrite = 0.145. Caudate body axo-spine = 0.0961; axo-dendrite = 0.0474. Pre-commissural putamen axo-spine = 0.066; axo-dendrite = 0.035. Post-commissural putamen axo-spine = 0.516; axo-dendrite = 0.486

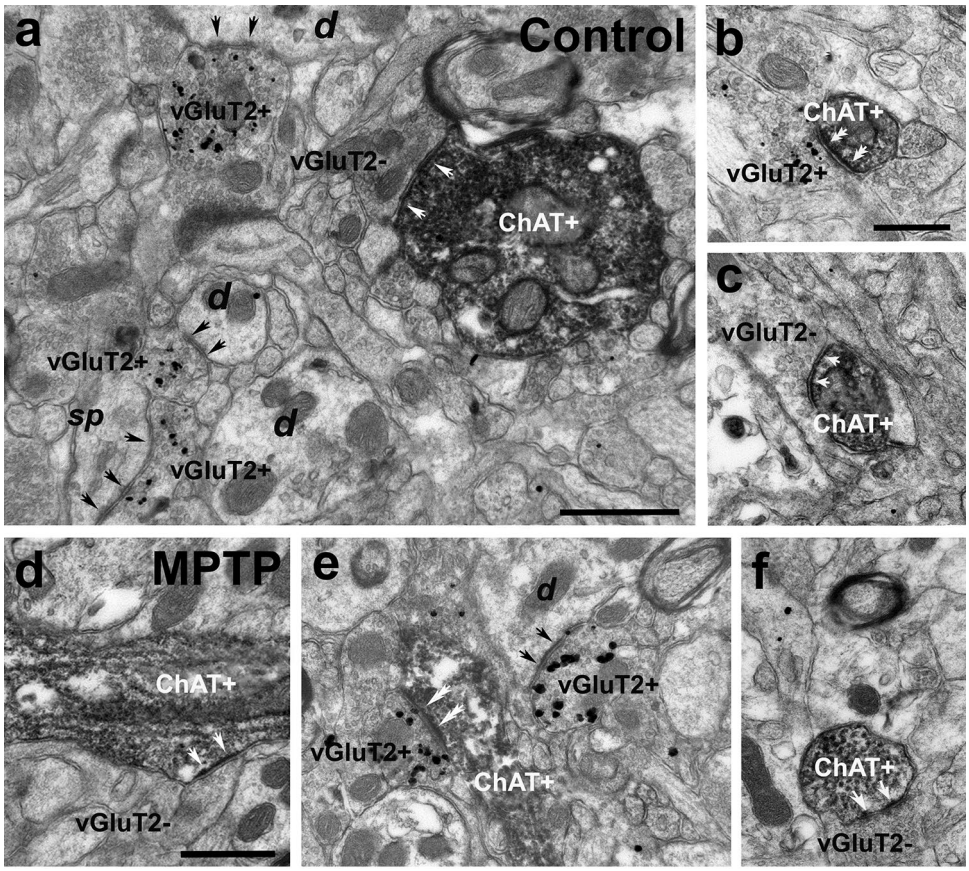

Fig. 6 Electron micrographs of ChAT-immunostained (peroxidase) dendrites and vGluT2-immunolabeled (silver-intensified gold particles) terminals in the putamen (**a**, **b**, **d**, **e**) and caudate (**c**, **f**) of control (**a**, **b**, **c**) and MPTP-treated monkeys (**d**, **e**, **f**). **a** A large-sized ChAT + dendrite (diameter > 1 µm) forms an asymmetric synapse (white arrows) with a vGluT2-negative (vGluT2−) terminal. In the same field, some vGluT2-positive (vGluT2+) terminals form asymmetric synapses (black arrows) with non-labeled dendrites (d) and a dendritic spine (sp). **b** A vGluT2 + terminal forms an asymmetric synapse with a small-sized (diameter < 0.5 µm) ChAT + dendrite (double white arrows). **c** Medium-sized (diameter between 0.5 and 1 µm) ChAT-immunostained dendrite receiving an asymmetric synapse from a vGluT2-negative (white arrows). Large- (**d**) and medium-sized (**e**, **f**) ChAT + dendrites form asymmetric synapses with vGluT2- (white arrows in **d** and **f**) and vGluT2 + (double white arrows in e) terminals. Scale bars in **a** = 0.5 µm, in **b** (applies to **c**) = 0.5 µm and in **d** = 0.5 µm (applies to **d** and **f**)

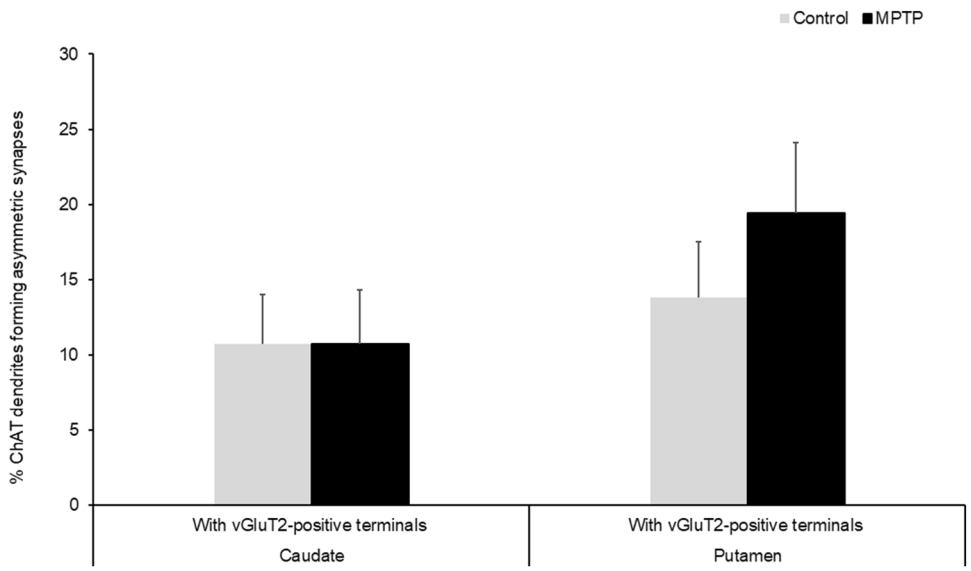

Fig. 7 Histograms comparing the percentages of ChAT-positive dendrites that form asymmetric synapses with vGluT2-positive terminals in the caudate and putamen of control and MPTP-treated monkeys. In both the caudate and putamen, no significant differences (Chi square test) between control and parkinsonian monkeys were found in the proportions of ChAT-positive dendrites receiving vGluT2-positive terminals

conclusions can be drawn from our observations: (1) as reported in PD patients and in our previous monkey study, CM/Pf neurons undergo profound degeneration in monkeys chronically treated with low doses of MPTP (Villalba et al. 2014; Smith et al. 2014a), which further validate the use of the chronic MPTP-treated monkey model of PD to study potential motor and non-motor signs associated with CM/Pf neuronal degeneration in PD (Smith et al. 2014b; Masilamoni and Smith 2018). (2) Albeit they did not reach significance, modest changes in volume and in total number of ChIs were found in the caudate nucleus and putamen of chronically MPTP-treated monkeys. Together, these changes led to an increased density of ChIs in the caudate nucleus (head and body) of parkinsonian monkeys. (3) Despite the robust loss of CM/Pf neurons, no significant change was found in the density of vGluT2-positive thalamostriatal terminals and in the prevalence of vGluT2 terminals in contact with ChIs in parkinsonian monkeys. Thus, in spite of a profound CM/Pf degeneration, the overall anatomy of the synaptic relationships between thalamic terminals (as revealed with vGluT2) and striatal ChIs is not significantly altered in parkinsonian monkeys. In the following account, the functional significance of these observations, and the potential neuroplastic changes that may underlie possible differences between the extent of CM/Pf neuronal loss and the degree of thalamostriatal denervation will be discussed.

CM/Pf degeneration in Parkinson's disease and chronically MPTP-treated monkeys

As previously reported in PD patients, and in our previous study (Henderson et al. 2000a, b, 2005; Brooks and Halliday 2009; Halliday and Stevens 2011; Villalba et al. 2014; Smith et al. 2014b), the present findings demonstrate that rhesus monkeys chronically treated with low doses of the neurotoxin MPTP displayed robust CM/Pf neuronal loss. Although the present study did not attempt at assessing the relationships between the extent of CM/Pf cell loss and the severity of parkinsonian motor symptoms, our recent findings indicated that the loss of CM/Pf neurons is an early pathology that reaches its maximal extent (~40 to 50%) prior to the development of parkinsonian motor symptoms in chronically MPTP-treated monkeys (Villalba et al. 2014). Consistent with these observations, human postmortem studies indicated that the degree of neuronal loss in CM/Pf was the same in early diagnosed vs late, severely disabled, PD patients (Henderson et al. 2000a, b, 2005; Brooks and Halliday 2009; Halliday and Stevens 2011). Together, these observations indicate that CM/Pf neurodegeneration in PD is unrelated to the severity of PD motor signs, but rather contributes to early non-motor features of the disease (Smith et al. 2014a). Although cell loss was also found in some rostral intralaminar nuclei, the CM/Pf is, by far, the most affected thalamic nuclear group in PD patients (Henderson et al. 2000a, b; Halliday 2009). In chronically MPTP-treated monkeys, no significant cell loss was found in the mediodorsal nucleus, despite its close proximity to the CM/Pf complex (Villalba et al. 2014). Thus, a subset of CM/Pf neurons appears to be particularly sensitive to degeneration in PD and in response to chronic treatment with MPTP. Whether chronic MPTP toxicity and PD pathology target the same CM/Pf neurons in monkeys and humans remain to be established. However, the fact that the extent of neuronal loss is closely similar, and that the CM/Pf pathology is an early event unrelated to the severity of parkinsonian motor symptoms in both MPTP-treated monkeys and PD patients, strongly suggests that the same neuronal groups may be targeted in human and nonhuman primates. In humans, Halliday and colleagues reported that CM/Pf parvalbumin-negative neurons are more severely affected than parvalbumin-positive cells in PD (Truong et al. 2009; Henderson et al. 2000a), suggesting that differential calcium-buffering capabilities may partly underlie the susceptibility of specific CM/Pf neurons to degeneration in PD. In that regard, the complete lack of calbindin expression in CM/Pf neurons (Parent et al. 1996; Henderson et al. 2000a; Munkle et al. 2000; Smith et al. 2014b; Villalba et al. 2014) may make this nuclear group more sensitive than other thalamic regions in PD or in response to MPTP-induced toxicity (Iacopino et al. 1992; Liang et al. 1996; Yuan et al. 2013; Dopeso-Reyes et al. 2014; Spruill and Kuncl 2015). Another distinctive feature of CM/Pf neurons is their preferential expression of different proteins such as cerebellin 1, leucine-rich repeat containing GPCR8 (LGR8) and Frizzled5 compared with other thalamic neurons (Shen et al. 2005; Liu et al. 2008; Sedaghat et al. 2009; Kusnoor et al. 2010). Whether dysregulation of these proteins contributes to PD pathology of CM/Pf remains to be examined. The cellular mechanisms through which chronic MPTP administration results in CM/Pf cell also remain enigmatic. Although evidence of chronic MPTP (and MPP+)-induced toxicity in various monoaminergic cell groups has been reported (Altar et al. 1986; Singer et al. 1988; Herkenham et al. 1991; Johannessen 1991; Przedborski et al. 2000; Watanabe et al. 2005; Fornai et al. 2005; Masilamoni et al. 2011; Masilamoni and Smith 2018), the neurotoxic impact of MPTP or MPP+ upon non-monoaminergic neurons remains scant. However, it is noteworthy that intrastriatal injection of MPP+ or systemic injection of MPTP induces significant neuronal loss in Pf and SNc, without any significant effect on cortical neurons (Freyaldenhoven et al. 1997; Ghorayeb et al. 2002), suggesting that Pf neurons, such as midbrain dopaminergic cells, are highly vulnerable to MPTP toxicity. Some authors have also reported loss of Pf neurons in the unilateral 6-OHDA-treated rodent model of PD (Aymerich et al. 2006), but others did not (Kusnoor et al. 2012; Parker et al. 2016). Although the sources of these variable results

remain unclear, the lack of thalamic degeneration in some rodent models of PD raise concerns about the reliability of such animal models to study functional changes of the thalamostriatal system in human PD (Villalba and Smith 2018).

CM/Pf neuronal loss versus thalamostriatal degeneration

Because the caudal intralaminar complex is one of the main sources of the thalamostriatal system (see Smith et al. 2004, 2011, 2014b for reviews) in primates, the profound degeneration of CM/Pf neurons in MPTP-treated monkeys (and in PD patients) could lead to significant thalamic denervation of the striatum in the parkinsonian state. However, our EM findings suggest otherwise, i.e. no significant change in the prevalence of vGluT2-immunoreactive terminals was found in the putamen of MPTP-treated parkinsonian monkeys with robust CM/Pf neuronal loss. Although these observations may appear paradoxical, various compensatory neuroplastic changes may explain such a dichotomy: (1) other thalamic nuclei may homeostatically increase their striatal innervation to relieve the progressive loss of CM/Pf-striatal terminals. Knowing that many thalamic nuclei contribute to the thalamostriatal innervation (Berendse and Groenewegen 1990; Sidibe and Smith 1999; Smith et al. 2004, 2009, 2014a), and that most vGluT2-containing terminals in the normal striatum have a non-CM/Pf origin (Raju et al. 2006), an homeostatic or maladaptive sprouting of vGluT2-positive axonal projections to compensate for the loss of vGluT2 CM/Pf terminals should be considered, (2) the CM/Pf-striatal neurons spared by the MPTP-induced toxicity increase their striatal innervation to compensate for the loss of thalamic terminals induced by CM/Pf neuronal death. Although as much as ~ 40–50% CM/Pf neurons undergo degeneration in MPTP-treated parkinsonian monkeys and PD patients, more than half CM/Pf neurons are spared. Although the exact projection sites and potential changes in the extent of striatal innervation of the remaining CM/Pf neurons in parkinsonian monkeys and PD patients remain unknown, previous rodent studies support this possibility. In 6-OHDA-treated rats with partial Pf degeneration, a subset of spared Pf neurons were, indeed, identified as Pf-striatal neurons with increased vGluT2 mRNA expression, suggesting a compensatory increased activity in the parkinsonian condition (Aymerich et al. 2006; see also Bacci et al. 2002, 2004), (3) an increased volume of remaining vGluT2-containing terminals in the striatum of parkinsonian monkeys may partly compensate for the loss of vGluT2-positive terminal profiles counted from single ultrathin sections. Our recent findings have, indeed, shown a significant increase in the volume of thalamic and cortical terminals in the striatum of MPTP-treated parkinsonian monkeys (Villalba and Smith 2010, 2011, 2018). However, although this possibility could not be completely ruled out, the fact that vGluT2 terminal profile counts in the present study were achieved from single ultra-thin sections spaced apart by at least 1–2 µm reduce the likelihood that the same terminals were counted twice in our analysis, (4) most CM/Pf neurons that undergo degeneration in MPTP-treated monkeys do not project to the striatum, but rather give rise to cortical innervation. Although a majority of CM/Pf neurons project to the striatum, a subset of CM/Pf cells project solely to the cerebral cortex (Smith and Parent 1986; Sadikot et al. 1992a, b; Parent and Parent 2005). Our recent evidence for partial vGluT2 denervation of deep layers in M1 of MPTP-treated monkeys (Villalba et al. 2018) is in line with this possibility, (5) a subset of thalamostriatal terminals from CM/Pf do not express vGluT2 immunoreactivity. Although unlikely, it is noteworthy that ~ 20% putative glutamatergic terminals in the primate and rodent striatum do not express vGluT1 or vGluT2 immunostaining (Lacey et al. 2005; Raju et al. 2008). Whether a subset of these terminals originates from CM/Pf, and may be lost in the parkinsonian state, remains to be established.

Thus, it appears that a deeper understanding of the neuroplastic properties of thalamostriatal projections and further knowledge of the anatomy of degenerated vs spared CM/Pf neurons in parkinsonian monkeys are warranted to fully elucidate the underlying substrate of differences between the extent of CM/Pf degeneration and the lack of significant thalamic denervation in parkinsonian condition.

CM/Pf innervation of striatal cholinergic interneurons in normal and parkinsonian condition

Cholinergic interneurons (ChIs) are key constituents of the striatal microcircuitry that have been recognized as central nodes for the processing of attentional salient stimuli in the context of reward-related behaviors (Aosaki et al. 1994; Pisani et al. 2001; Ravel et al. 2003; Kimura et al. 2004; Morris et al. 2004; Joshua et al. 2008; Apicella et al. 2011; Bonsi et al. 2011). Their contribution to a wide array of motor and non-motor symptoms associated with various basal ganglia disorders has been recognized, making them a prime target for brain disease therapeutics (Pisani et al. 2003, 2007; Chung et al. 2010; Ding et al. 2011; Quik et al. 2014; Won et al. 2014; Zhang et al. 2014; Maurice et al. 2015; Bordia et al. 2016; Tanimura et al. 2019). Their extensive dendritic and axonal arbors allow to integrate and transmit information across functionally diverse striatal territories (Gonzales and Smith 2015; Abudukeyoumu et al. 2019). Dopaminergic, GABAergic and glutamatergic afferents are important regulators of their physiological responses to attentional stimuli (Schultz et al. 1993; Minamimoto and Kimura 2002; Kimura et al. 2004; Morris et al. 2004; Gibbs et al. 2007; Joshua et al. 2008; Nanda et al. 2009; Apicella et al.

2011; Bonsi et al. 2011; Gonzales et al. 2013; Anderson et al. 2016; Assous and Tepper 2019). More specifically, the CM/Pf is the main source of extrinsic glutamatergic drive to these neurons (Akins et al. 1990; Meredith and Wouterlood 1990; Lapper and Bolam 1992; Sidibe and Smith 1999; Ding et al. 2010; Brown et al. 2010; Galvan and Smith 2011; Smith et al. 2014a). In mice, disruption of the functional connection between the Pf and ChIs in the dorsomedial striatum significantly hampers goal-directed actions and executive control (Bradfield et al. 2013; Hart et al. 2014; Smith et al. 2014a; Matamales et al. 2016; Balleine et al. 2007; Bradfield and Balleine 2017; Saund et al. 2017; Yamanaka et al. 2018; Wolff and Vann 2019). In rhesus monkeys, blockade of CM/Pf activity induces significant changes in the pattern of ChI responses to attentional stimuli (Minamimoto and Kimura 2002; Nanda et al. 2009; Brown et al. 2010). Combined with additional CM/Pf-striatal lesion studies and case reports of human CM/Pf infarcts that led to cognitive impairments in behavioral flexibility and attention, these data strongly suggest that the CM/Pf-striatal system, in part through its interactions with striatal ChIs, is a key regulator of complex basal ganglia-mediated cognitive behaviors (see Smith et al. 2011, 2014a; Balleine et al. 2015; Peak et al. 2019 for reviews). In that regard, our findings that striatal ChIs do not undergo a significant thalamic denervation despite major neuronal loss in CM/Pf of parkinsonian monkeys are highly relevant, because these may be indicative that the CM/Pf-ChIs connection remains intact in the brain of PD patients despite loss of thalamic cells. However, other alternative explanations must be considered. The various neuroplastic changes discussed in the previous section to explain the limited change in the prevalence of striatal vGluT2 terminals in parkinsonian monkeys also apply to the thalamic innervation of ChIs. In addition, one could also raise the possibility that the CM/Pf innervation of ChIs originates from a specific subset of CM/Pf neurons, different from those that innervate striatal projection neurons, which are selectively spared in parkinsonian monkeys. A detailed characterization of the fine microcircuitry and exact cellular sources of CM/Pf terminals in contact with specific striatal interneuron and projection neuron subtypes is needed to fully elucidate this issue. To further address the functional significance of these anatomic observations, electrophysiological responses of putative striatal ChIs to CM/Pf stimulation in control and parkinsonian monkeys are needed. In line with recent findings from another group, our stereological analysis of ChI counts did not reveal any statistically significant differences in the total number of striatal ChIs (ChAT-IR) between control and parkinsonian monkeys (Petryszyn et al. 2016).

Technical limitations

Some potential limitations inherent to the use of immuno-EM approaches must be considered in the interpretation of our data. The possibility that the lack of change in the prevalence of vGluT2 terminals in the putamen of parkinsonian monkeys resulted from the variable penetration of vGluT2 antibodies through the striatal tissue between control and parkinsonian monkeys cannot be completely ruled out, though unlikely to be a major contributor to our observations, because care was taken in sampling vGluT2 terminals solely from the very superficial sections of tissue blocks where the antibodies penetration is optimal in both groups of animals. The fact that the variability of results from individual monkey in the control and parkinsonian group was low demonstrates the consistency and reliability of findings between and across experimental groups. Furthermore, because the use of a similar quantitative approach allowed us to demonstrate a decrease in the prevalence of vGluT1 terminals in the subthalamic nucleus of parkinsonian monkeys in our recent study (Mathai et al. 2015) validates the sampling strategy to address the current issue. Another consideration is the fact that unbiased stereological approach for vGluT2 terminal counts was not used in the present study. Although we understand that this would have been the optimal method to use, our material was not suitable for such a quantitative analysis. Thus, as an alternative, we quantified the density of boutons based on counts of terminal profiles from serial ultrathin sections far enough from each other to avoid counting the same profile twice. The use of this sampling approach, combined with the fact that only the most superficial ultrathin sections of tissue blocks were analyzed to ensure optimal vGluT2 immunostaining, the limited variability of results in terminal profile counts between individual monkeys of the same or different groups, and results of our previous STN study showing vGluT1 terminal loss using a similar EM approach, make us confident that findings reported in the present work lay on a solid foundation and indicate a genuine lack of significant vGluT2 terminal loss in the striatum of MPTP-treated monkeys. The lack of change in the proportion of thalamic terminals in contact with ChIs in parkinsonian monkeys also deserves some consideration. To increase the likelihood of contacts between vGuT2 terminals and ChAT-positive elements, we collected data for this part of the study only from striatal regions that expressed both markers in the close vicinity of each other. In doing so, we ensured that the areas under analysis were exposed to both antibodies, avoiding false negative labeling due to poor antibody penetration. To make sure the thalamic innervation of all parts of ChAT neurons was examined, we specifically looked at the vGluT2 innervation of large-, medium- and small-sized dendrites. This allowed us to determine if changes of vGluT2 innervation might have affected

proximal or distal parts of the ChIs dendritic trees. It is also critical to mention that all EM data collected in this study were done in a blinded fashion, i.e. the investigator collecting the EM data was blinded to the animal group under study until all EM data had been gathered and tabulated.

Thus, overall, we feel confident that the data presented in this study provide an unbiased view of the state of thalamic innervation of the striatum in parkinsonian monkeys with CM/Pf degeneration. Because Cre-expressing transgenic monkeys are not yet available, some of the modern techniques used in mice to trace monosynaptic inputs to specific subsets of neurons (Ginger et al. 2013; Wall et al. 2010; Callaway and Luo 2015; Guo et al. 2015) cannot be applied to the study of nonhuman primate functional microcircuits. Further development of such tracing method for use in primates could help confirm and expand our findings. Although neither EM nor viral-based tracing methods can be used in the human brain, a light or confocal microscopy analysis of the abundance vGluT2-positive terminal-like puncta in the striatum of control and parkinsonian patients is needed to assess the significance of our findings to the human diseased condition.

Concluding remarks

Although it long remained obscure, our understanding of the potential role of the CM/Pf-striatal connection in cognition uncovered during the past decade has rejuvenated interest for the thalamostriatal system (Kimura et al. 2004; Metzger et al. 2010; Bradfield et al. 2013; Saalmann 2014; Balleine et al. 2015; Bradfield and Balleine 2017; Melief et al. 2018; Yamanaka et al. 2018; Wolff and Vann 2019). In particular, the close functional link between the CM/Pf and ChIs is now seen as key functional network involved in the regulation of goal-directed actions and behavioral flexibility. These behavioral observations, combined with the fact that the CM/Pf undergoes profound degeneration in PD, raise some interesting possibilities about the potential contribution of the CM/Pf-striatal degeneration in cognitive impairments related to executive function in PD (see Schneider and Kovelowski 1990; Smith et al. 2011, 2014a; Solari et al. 2013; Balleine et al. 2015 and Peak et al. 2019 for reviews). The fact that CM/Pf neuronal loss is an early pathology in PD patients and chronically MPTP-treated monkeys suggests that functional consequences of thalamic degeneration might occur early in PD, most likely prior to the development of parkinsonian motor features. Early executive dysfunction in attentional set-shifting have, indeed, been reported in early diagnosed PD patients and in motor asymptomatic MPTP-treated monkeys chronically treated with low doses of MPTP (Slovin et al. 1999; Pessiglione et al. 2003; Maiti et al. 2016). Whether these cognitive impairments result from degeneration of the CM/Pf-striatal system is unknown, but surely worth considering because the main projection site of CM/Pf neurons is the dorsal striatum (Sidibe and Smith 1999; Smith et al. 2009, 2014a; Galvan and Smith 2011; Melief et al. 2018). The findings of our study bring up an additional level of intricacy to the consequences of thalamic pathology upon the functional microcircuitry of the thalamostriatal system in parkinsonism. The limited changes seen in the relative prevalence and synaptic connections of thalamic terminals with ChIs in MPTP-treated monkeys raise the possibility that the CM/Pf lesion may not have a significant impact upon the functional role of the CM/Pf-striatal system in PD. Alternatively, our observations may suggest that the CM/Pf degeneration leads to a cascade of compensatory or maladaptive neuroplastic changes that result in a complex reorganization and axonal sprouting of other thalamic inputs to the striatum. Future anatomical and functional studies aimed at assessing the functional impact of CM/Pf and other thalamic nuclei activation upon ChIs and striatal projection neurons in control and parkinsonian monkeys are needed to further address these issues.

Acknowledgements The authors thank Susan Jenkins for technical assistance. We also thank Dr. Kalynda Gonzales for her constructive inputs and discussions about part of the work presented in this manuscript. This work was supported by NIH Grants (R01NS083386; P50NS098685) and the NIH/ORIP P51 NIH base Grant (P51OD011132) of the Yerkes National Primate Research Center.

Funding This study was funded by the National Institutes of Health (NIH, USA) Grants (R01NS083386; P50NS098685) and the NIH/ORIP P51 NIH base Grant (P51OD011132) of the Yerkes National Primate Research Center.

Compliance with ethical standards

Conflict of interest The authors declared that they have no conflict of interest.

Ethical approval This article does not contain any studies with human participants performed by any of the authors. All procedures performed in studies involving animals were in accordance with the ethical standards. The housing, feeding, and experimental conditions used in these studies followed the guidelines by the National Institutes of Health, and are approved by Emory University's Institutional Animal Care and Use Committee (IACUC).

References

Abudukeyoumu N, Hernandez-Flores T, Garcia-Munoz M, Arbuthnott GW (2019) Cholinergic modulation of striatal microcircuits. Eur J Neurosci 49:604–622

Akins PT, Surmeier DJ, Kitai ST (1990) Muscarinic modulation of a transient K+ conductance in rat neostriatal neurons. Nature 344:240–242

Altar CA, Heikkila RE, Manzino L, Marien MR (1986) 1-Methyl-4-phenylpyridine (MPP+): regional dopamine neuron uptake,

toxicity, and novel rotational behavior following dopamine receptor proliferation. Eur J Pharmacol 131:199–209
Anderson BA, Kuwabara H, Wong DF, Gean EG, Rahmim A, Brasic JR, George N, Frolov B, Courtney SM, Yantis S (2016) The role of dopamine in value-based attentional orienting. Curr Biol 26:550–555
Aosaki T, Tsubokawa H, Ishida A, Watanabe K, Graybiel AM, Kimura M (1994) Responses of tonically active neurons in the primate's striatum undergo systematic changes during behavioral sensorimotor conditioning. J Neurosci 14:3969–3984
Aosaki T, Miura M, Suzuki T, Nishimura K, Masuda M (2010) Acetylcholine-dopamine balance hypothesis in the striatum: an update. Geriatr Gerontol Int 10(Suppl 1):S148–S157
Apicella P, Ravel S, Deffains M, Legallet E (2011) The role of striatal tonically active neurons in reward prediction error signaling during instrumental task performance. J Neurosci 31:1507–1515
Assous M, Tepper JM (2019) Excitatory extrinsic afferents to striatal interneurons and interactions with striatal microcircuitry. Eur J Neurosci 49:593–603
Aymerich MS, Barroso-Chinea P, Perez-Manso M, Munoz-Patino AM, Moreno-Igoa M, Gonzalez-Hernandez T, Lanciego JL (2006) Consequences of unilateral nigrostriatal denervation on the thalamostriatal pathway in rats. Eur J Neurosci 23:2099–2108
Bacci JJ, Kerkerian-Le Goff L, Salin P (2002) Effects of intralaminar thalamic nuclei lesion on glutamic acid decarboxylase (GAD65 and GAD67) and cytochrome oxidase subunit I mRNA expression in the basal ganglia of the rat. Eur J Neurosci 15:1918–1928
Bacci JJ, Kachidian P, Kerkerian-Le Goff L, Salin P (2004) Intralaminar thalamic nuclei lesions: widespread impact on dopamine denervation-mediated cellular defects in the rat basal ganglia. J Neuropathol Exp Neurol 63:20–31
Balleine BW, Delgado MR, Hikosaka O (2007) The role of the dorsal striatum in reward and decision-making. J Neurosci 27:8161–8165
Balleine BW, Morris RW, Leung BK (2015) Thalamocortical integration of instrumental learning and performance and their disintegration in addiction. Brain Res 1628:104–116
Berendse HW, Groenewegen HJ (1990) Organization of the thalamostriatal projections in the rat, with special emphasis on the ventral striatum. J Comp Neurol 299:187–228
Bernacer J, Prensa L, Gimenez-Amaya JM (2007) Cholinergic interneurons are differentially distributed in the human striatum. PLoS One 2:e1174
Bernacer J, Prensa L, Gimenez-Amaya JM (2012) Distribution of GABAergic interneurons and dopaminergic cells in the functional territories of the human striatum. PLoS One 7:e30504
Bonsi P, Cuomo D, Martella G, Madeo G, Schirinzi T, Puglisi F, Ponterio G, Pisani A (2011) Centrality of striatal cholinergic transmission in Basal Ganglia function. Front Neuroanat 5:6
Bordia T, Perez XA, Heiss J, Zhang D, Quik M (2016) Optogenetic activation of striatal cholinergic interneurons regulates L-dopa-induced dyskinesias. Neurobiol Dis 91:47–58
Bradfield LA, Balleine BW (2017) Thalamic control of dorsomedial striatum regulates internal state to guide goal-directed action selection. J Neurosci 37:3721–3733
Bradfield LA, Bertran-Gonzalez J, Chieng B, Balleine BW (2013) The thalamostriatal pathway and cholinergic control of goal-directed action: interlacing new with existing learning in the striatum. Neuron 79:153–166
Brooks D, Halliday GM (2009) Intralaminar nuclei of the thalamus in Lewy body diseases. Brain Res Bull 78:97–104
Brown HD, Baker PM, Ragozzino ME (2010) The parafascicular thalamic nucleus concomitantly influences behavioral flexibility and dorsomedial striatal acetylcholine output in rats. J Neurosci 30:14390–14398
Callaway EM, Luo L (2015) Monosynaptic circuit tracing with glycoprotein-deleted rabies viruses. J Neurosci 35:8979–8985
Chung KA, Lobb BM, Nutt JG, Horak FB (2010) Effects of a central cholinesterase inhibitor on reducing falls in Parkinson disease. Neurology 75:1263–1269
Deng YP, Wong T, Bricker-Anthony C, Deng B, Reiner A (2013) Loss of corticostriatal and thalamostriatal synaptic terminals precedes striatal projection neuron pathology in heterozygous Q140 Huntington's disease mice. Neurobiol Dis 60:89–107
DiFiglia M (1987) Synaptic organization of cholinergic neurons in the monkey neostriatum. J Comp Neurol 255:245–258
Ding JB, Guzman JN, Peterson JD, Goldberg JA, Surmeier DJ (2010) Thalamic gating of corticostriatal signaling by cholinergic interneurons. Neuron 67:294–307
Ding Y, Won L, Britt JP, Lim SA, McGehee DS, Kang UJ (2011) Enhanced striatal cholinergic neuronal activity mediates L-DOPA-induced dyskinesia in parkinsonian mice. Proc Natl Acad Sci USA 108:840–845
Dopeso-Reyes IG, Rico AJ, Roda E, Sierra S, Pignataro D, Lanz M, Sucunza D, Chang-Azancot L, Lanciego JL (2014) Calbindin content and differential vulnerability of midbrain efferent dopaminergic neurons in macaques. Front Neuroanat 8:146
Fornai F, Schluter OM, Lenzi P, Gesi M, Ruffoli R, Ferrucci M, Lazzeri G, Busceti CL, Pontarelli F, Battaglia G, Pellegrini A, Nicoletti F, Ruggieri S, Paparelli A, Sudhof TC (2005) Parkinson-like syndrome induced by continuous MPTP infusion: convergent roles of the ubiquitin-proteasome system and alpha-synuclein. Proc Natl Acad Sci USA 102:3413–3418
Fremeau RT Jr, Troyer MD, Pahner I, Nygaard GO, Tran CH, Reimer RJ, Bellocchio EE, Fortin D, Storm-Mathisen J, Edwards RH (2001) The expression of vesicular glutamate transporters defines two classes of excitatory synapse. Neuron 31:247–260
Freyaldenhoven TE, Ali SF, Schmued LC (1997) Systemic administration of MPTP induces thalamic neuronal degeneration in mice. Brain Res 759:9–17
Galvan A, Smith Y (2011) The primate thalamostriatal systems: anatomical organization, functional roles and possible involvement in Parkinson's disease. Basal Ganglia 1:179–189
Gerfen CR, Engber TM, Mahan LC, Susel Z, Chase TN, Monsma FJ Jr, Sibley DR (1990) D1 and D2 dopamine receptor-regulated gene expression of striatonigral and striatopallidal neurons. Science 250:1429–1432
Ghorayeb I, Fernagut PO, Hervier L, Labattu B, Bioulac B, Tison F (2002) A 'single toxin-double lesion' rat model of striatonigral degeneration by intrastriatal 1-methyl-4-phenylpyridinium ion injection: a motor behavioural analysis. Neuroscience 115:533–546
Gibbs AA, Naudts KH, Spencer EP, David AS (2007) The role of dopamine in attentional and memory biases for emotional information. Am J Psychiatry 164:1603–1609 **(quiz 1624)**
Ginger M, Haberl M, Conzelmann KK, Schwarz MK, Frick A (2013) Revealing the secrets of neuronal circuits with recombinant rabies virus technology. Front Neural Circuits 7:2
Glaser EM, Wilson PD (1998) The coefficient of error of optical fractionator population size estimates: a computer simulation comparing three estimators. J Microsc 192:163–171
Gonzales KK, Smith Y (2015) Cholinergic interneurons in the dorsal and ventral striatum: anatomical and functional considerations in normal and diseased conditions. Ann N Y Acad Sci 1349:1–45
Gonzales KK, Pare JF, Wichmann T, Smith Y (2013) GABAergic inputs from direct and indirect striatal projection neurons onto cholinergic interneurons in the primate putamen. J Comp Neurol 521:2502–2522
Gundersen HJ (1986) Stereology of arbitrary particles. A review of unbiased number and size estimators and the presentation

of some new ones, in memory of William R. Thompson. J Microsc 143:3–45
Gundersen HJ, Osterby R (1981) Optimizing sampling efficiency of stereological studies in biology: or 'do more less well!'. J Microsc 121:65–73
Guo Q, Wang D, He X, Feng Q, Lin R, Xu F, Fu L, Luo M (2015) Whole-brain mapping of inputs to projection neurons and cholinergic interneurons in the dorsal striatum. PLoS One 10:e0123381
Halliday GM (2009) Thalamic changes in Parkinson's disease. Parkinsonism Relat Disord 15(Suppl 3):S152–S155
Halliday GM, Stevens CH (2011) Glia: initiators and progressors of pathology in Parkinson's disease. Mov Disord 26:6–17
Halliday GM, Macdonald V, Henderson JM (2005) A comparison of degeneration in motor thalamus and cortex between progressive supranuclear palsy and Parkinson's disease. Brain 128:2272–2280
Hart G, Leung BK, Balleine BW (2014) Dorsal and ventral streams: the distinct role of striatal subregions in the acquisition and performance of goal-directed actions. Neurobiol Learn Mem 108:104–118
Henderson JM, Carpenter K, Cartwright H, Halliday GM (2000a) Degeneration of the centre median-parafascicular complex in Parkinson's disease. Ann Neurol 47:345–352
Henderson JM, Carpenter K, Cartwright H, Halliday GM (2000b) Loss of thalamic intralaminar nuclei in progressive supranuclear palsy and Parkinson's disease: clinical and therapeutic implications. Brain 123(Pt 7):1410–1421
Henderson JM, Schleimer SB, Allbutt H, Dabholkar V, Abela D, Jovic J, Quinlivan M (2005) Behavioural effects of parafascicular thalamic lesions in an animal model of parkinsonism. Behav Brain Res 162:222–232
Herkenham M, Little MD, Bankiewicz K, Yang SC, Markey SP, Johannessen JN (1991) Selective retention of MPP+ within the monoaminergic systems of the primate brain following MPTP administration: an in vivo autoradiographic study. Neuroscience 40:133–158
Iacopino A, Christakos S, German D, Sonsalla PK, Altar CA (1992) Calbindin-D28K-containing neurons in animal models of neurodegeneration: possible protection from excitotoxicity. Brain Res Mol Brain Res 13:251–261
Johannessen JN (1991) A model of chronic neurotoxicity: long-term retention of the neurotoxin 1-methyl-4-phenylpyridinium (MPP+) within catecholaminergic neurons. Neurotoxicology 12:285–302
Joshua M, Adler A, Mitelman R, Vaadia E, Bergman H (2008) Midbrain dopaminergic neurons and striatal cholinergic interneurons encode the difference between reward and aversive events at different epochs of probabilistic classical conditioning trials. J Neurosci 28:11673–11684
Kawaguchi Y, Wilson CJ, Augood SJ, Emson PC (1995) Striatal interneurones: chemical, physiological and morphological characterization. Trends Neurosci 18:527–535
Kimura M, Minamimoto T, Matsumoto N, Hori Y (2004) Monitoring and switching of cortico-basal ganglia loop functions by the thalamo-striatal system. Neurosci Res 48:355–360
Kusnoor SV, Parris J, Muly EC, Morgan JI, Deutch AY (2010) Extracerebellar role for Cerebellin1: modulation of dendritic spine density and synapses in striatal medium spiny neurons. J Comp Neurol 518:2525–2537
Kusnoor SV, Bubser M, Deutch AY (2012) The effects of nigrostriatal dopamine depletion on the thalamic parafascicular nucleus. Brain Res 1446:46–55
Lacey CJ, Boyes J, Gerlach O, Chen L, Magill PJ, Bolam JP (2005) GABA(B) receptors at glutamatergic synapses in the rat striatum. Neuroscience 136:1083–1095
Lallani SB, Villalba RM, Chen Y, Smith Y, Chan A (2019) Striatal interneurons in transgenic nonhuman primate model of Huntington's disease. Nature. Scientific Reports 9, Article number: 3528
Lanciego JL, Luquin N, Obeso JA (2012) Functional neuroanatomy of the basal ganglia. Cold Spring Harb Perspect Med 2:a009621
Lapper SR, Bolam JP (1992) Input from the frontal cortex and the parafascicular nucleus to cholinergic interneurons in the dorsal striatum of the rat. Neuroscience 51:533–545
Liang CL, Sinton CM, German DC (1996) Midbrain dopaminergic neurons in the mouse: co-localization with Calbindin-D28K and calretinin. Neuroscience 75:523–533
Liu C, Wang Y, Smallwood PM, Nathans J (2008) An essential role for Frizzled5 in neuronal survival in the parafascicular nucleus of the thalamus. J Neurosci 28:5641–5653
Maiti P, Gregg LC, McDonald MP (2016) MPTP-induced executive dysfunction is associated with altered prefrontal serotonergic function. Behav Brain Res 298:192–201
Masilamoni GJ, Smith Y (2018) Chronic MPTP administration regimen in monkeys: a model of dopaminergic and non-dopaminergic cell loss in Parkinson's disease. J Neural Transm (Vienna) 125:337–363
Masilamoni G, Votaw J, Howell L, Villalba RM, Goodman M, Voll RJ, Stehouwer J, Wichmann T, Smith Y (2010) (18)F-FECNT: validation as PET dopamine transporter ligand in parkinsonism. Exp Neurol 226:265–273
Masilamoni GJ, Bogenpohl JW, Alagille D, Delevich K, Tamagnan G, Votaw JR, Wichmann T, Smith Y (2011) Metabotropic glutamate receptor 5 antagonist protects dopaminergic and noradrenergic neurons from degeneration in MPTP-treated monkeys. Brain 134:2057–2073
Matamales M, Skrbis Z, Hatch RJ, Balleine BW, Gotz J, Bertran-Gonzalez J (2016) Aging-related dysfunction of striatal cholinergic interneurons produces conflict in action selection. Neuron 90:362–373
Mathai A, Ma Y, Pare JF, Villalba RM, Wichmann T, Smith Y (2015) Reduced cortical innervation of the subthalamic nucleus in MPTP-treated parkinsonian monkeys. Brain 138:946–962
Maurice N, Liberge M, Jaouen F, Ztaou S, Hanini M, Camon J, Deisseroth K, Amalric M, Kerkerian-Le Goff L, Beurrier C (2015) Striatal cholinergic interneurons control motor behavior and basal ganglia function in experimental parkinsonism. Cell Rep 13:657–666
Melief EJ, McKinley JW, Lam JY, Whiteley NM, Gibson AW, Neumaier JF, Henschen CW, Palmiter RD, Bamford NS, Darvas M (2018) Loss of glutamate signaling from the thalamus to dorsal striatum impairs motor function and slows the execution of learned behaviors. NPJ Parkinsons Dis 4:23
Meredith GE, Wouterlood FG (1990) Hippocampal and midline thalamic fibers and terminals in relation to the choline acetyltransferase-immunoreactive neurons in nucleus accumbens of the rat: a light and electron microscopic study. J Comp Neurol 296:204–221
Mesulam MM, Mufson EJ, Levey AI, Wainer BH (1984) Atlas of cholinergic neurons in the forebrain and upper brainstem of the macaque based on monoclonal choline acetyltransferase immunohistochemistry and acetylcholinesterase histochemistry. Neuroscience 12:669–686
Metzger CD, Eckert U, Steiner J, Sartorius A, Buchmann JE, Stadler J, Tempelmann C, Speck O, Bogerts B, Abler B, Walter M (2010) High field FMRI reveals thalamocortical integration of segregated cognitive and emotional processing in mediodorsal and intralaminar thalamic nuclei. Front Neuroanat 4:138
Minamimoto T, Kimura M (2002) Participation of the thalamic CM–Pf complex in attentional orienting. J Neurophysiol 87:3090–3101

Morris G, Arkadir D, Nevet A, Vaadia E, Bergman H (2004) Coincident but distinct messages of midbrain dopamine and striatal tonically active neurons. Neuron 43:133–143

Munkle MC, Waldvogel HJ, Faull RL (2000) The distribution of calbindin, calretinin and parvalbumin immunoreactivity in the human thalamus. J Chem Neuroanat 19:155–173

Nanda B, Galvan A, Smith Y, Wichmann T (2009) Effects of stimulation of the centromedian nucleus of the thalamus on the activity of striatal cells in awake rhesus monkeys. Eur J Neurosci 29:588–598

Oorschot DE (1996) Total number of neurons in the neostriatal, pallidal, subthalamic, and substantia nigral nuclei of the rat basal ganglia: a stereological study using the cavalieri and optical disector methods. J Comp Neurol 366:580–599

Oorschot D (2013) The percentage of interneurons in the dorsal striatum of the rat, cat, monkey and human: a critique of the evidence. Basal Ganglia 3:19–24

Parent M, Parent A (2005) Single-axon tracing and three-dimensional reconstruction of centre median-parafascicular thalamic neurons in primates. J Comp Neurol 481:127–144

Parent A, Fortin M, Cote PY, Cicchetti F (1996) Calcium-binding proteins in primate basal ganglia. Neurosci Res 25:309–334

Parker PR, Lalive AL, Kreitzer AC (2016) Pathway-specific remodeling of thalamostriatal synapses in parkinsonian mice. Neuron 89:734–740

Peak J, Hart G, Balleine BW (2019) From learning to action: the integration of dorsal striatal input and output pathways in instrumental conditioning. Eur J Neurosci 49:658–671

Pessiglione M, Guehl D, Agid Y, Hirsch EC, Feger J, Tremblay L (2003) Impairment of context-adapted movement selection in a primate model of presymptomatic Parkinson's disease. Brain 126:1392–1408

Petryszyn S, Di Paolo T, Parent A, Parent M (2016) The number of striatal cholinergic interneurons expressing calretinin is increased in parkinsonian monkeys. Neurobiol Dis 95:46–53

Petryszyn S, Parent A, Parent M (2018) The calretinin interneurons of the striatum: comparisons between rodents and primates under normal and pathological conditions. J Neural Transm (Vienna) 125:279–290

Pisani A, Bonsi P, Picconi B, Tolu M, Giacomini P, Scarnati E (2001) Role of tonically-active neurons in the control of striatal function: cellular mechanisms and behavioral correlates. Prog Neuropsychopharmacol Biol Psychiatry 25:211–230

Pisani A, Bonsi P, Centonze D, Gubellini P, Bernardi G, Calabresi P (2003) Targeting striatal cholinergic interneurons in Parkinson's disease: focus on metabotropic glutamate receptors. Neuropharmacology 45:45–56

Pisani A, Bernardi G, Ding J, Surmeier DJ (2007) Re-emergence of striatal cholinergic interneurons in movement disorders. Trends Neurosci 30:545–553

Przedborski S, Jackson-Lewis V, Djaldetti R, Liberatore G, Vila M, Vukosavic S, Almer G (2000) The parkinsonian toxin MPTP: action and mechanism. Restor Neurol Neurosci 16:135–142

Quik M, Zhang D, Perez XA, Bordia T (2014) Role for the nicotinic cholinergic system in movement disorders; therapeutic implications. Pharmacol Ther 144:50–59

Raju DV, Shah DJ, Wright TM, Hall RA, Smith Y (2006) Differential synaptology of vGluT2-containing thalamostriatal afferents between the patch and matrix compartments in rats. J Comp Neurol 499:231–243

Raju DV, Ahern TH, Shah DJ, Wright TM, Standaert DG, Hall RA, Smith Y (2008) Differential synaptic plasticity of the corticostriatal and thalamostriatal systems in an MPTP-treated monkey model of parkinsonism. Eur J Neurosci 27:1647–1658

Ravel S, Legallet E, Apicella P (2003) Responses of tonically active neurons in the monkey striatum discriminate between motivationally opposing stimuli. J Neurosci 23:8489–8497

Saalmann YB (2014) Intralaminar and medial thalamic influence on cortical synchrony, information transmission and cognition. Front Syst Neurosci 8:83

Sadikot AF, Parent A, Francois C (1992a) Efferent connections of the centromedian and parafascicular thalamic nuclei in the squirrel monkey: a PHA-L study of subcortical projections. J Comp Neurol 315:137–159

Sadikot AF, Parent A, Smith Y, Bolam JP (1992b) Efferent connections of the centromedian and parafascicular thalamic nuclei in the squirrel monkey: a light and electron microscopic study of the thalamostriatal projection in relation to striatal heterogeneity. J Comp Neurol 320:228–242

Saund J, Dautan D, Rostron C, Urcelay GP, Gerdjikov TV (2017) Thalamic inputs to dorsomedial striatum are involved in inhibitory control: evidence from the five-choice serial reaction time task in rats. Psychopharmacology 234:2399–2407

Schafer MK, Weihe E, Erickson JD, Eiden LE (1995) Human and monkey cholinergic neurons visualized in paraffin-embedded tissues by immunoreactivity for VAChT, the vesicular acetylcholine transporter. J Mol Neurosci 6:225–235

Schmitz C, Hof PR (2005) Design-based stereology in neuroscience. Neuroscience 130:813–831

Schneider JS, Kovelowski CJ 2nd (1990) Chronic exposure to low doses of MPTP. I. Cognitive deficits in motor asymptomatic monkeys. Brain Res 519:122–128

Schultz W, Apicella P, Ljungberg T, Romo R, Scarnati E (1993) Reward-related activity in the monkey striatum and substantia nigra. Prog Brain Res 99:227–235

Sedaghat K, Finkelstein DI, Gundlach AL (2009) Effect of unilateral lesion of the nigrostriatal dopamine pathway on survival and neurochemistry of parafascicular nucleus neurons in the rat–evaluation of time-course and LGR8 expression. Brain Res 1271:83–94

Shen PJ, Fu P, Phelan KD, Scott DJ, Layfield S, Tregear GW, Bathgate RA, Gundlach AL (2005) Restricted expression of LGR8 in intralaminar thalamic nuclei of rat brain suggests a role in sensorimotor systems. Ann N Y Acad Sci 1041:510–515

Sidibe M, Smith Y (1999) Thalamic inputs to striatal interneurons in monkeys: synaptic organization and co-localization of calcium binding proteins. Neuroscience 89:1189–1208

Singer TP, Ramsay RR, McKeown K, Trevor A, Castagnoli NE Jr (1988) Mechanism of the neurotoxicity of 1-methyl-4-phenylpyridinium (MPP+), the toxic bioactivation product of 1-methyl-4-phenyl-1,2,3,6-tetrahydropyridine (MPTP). Toxicology 49:17–23

Slovin H, Abeles M, Vaadia E, Haalman I, Prut Y, Bergman H (1999) Frontal cognitive impairments and saccadic deficits in low-dose MPTP-treated monkeys. J Neurophysiol 81:858–874

Smith Y, Parent A (1986) Differential connections of caudate nucleus and putamen in the squirrel monkey (*Saimiri sciureus*). Neuroscience 18:347–371

Smith Y, Raju DV, Pare JF, Sidibe M (2004) The thalamostriatal system: a highly specific network of the basal ganglia circuitry. Trends Neurosci 27:520–527

Smith Y, Raju D, Nanda B, Pare JF, Galvan A, Wichmann T (2009) The thalamostriatal systems: anatomical and functional organization in normal and parkinsonian states. Brain Res Bull 78:60–68

Smith Y, Surmeier DJ, Redgrave P, Kimura M (2011) Thalamic contributions to Basal Ganglia-related behavioral switching and reinforcement. J Neurosci 31:16102–16106

Smith Y, Galvan A, Ellender TJ, Doig N, Villalba RM, Huerta-Ocampo I, Wichmann T, Bolam JP (2014a) The thalamostriatal system in normal and diseased states. Front Syst Neurosci 8:5

Smith Y, Wichmann T, DeLong MR (2014b) Corticostriatal and mesocortical dopamine systems: do species differences matter? Nat Rev Neurosci 15:63

Solari N, Bonito-Oliva A, Fisone G, Brambilla R (2013) Understanding cognitive deficits in Parkinson's disease: lessons from preclinical animal models. Learn Mem 20:592–600

Spruill MM, Kuncl RW (2015) Calbindin-D28K is increased in the ventral horn of spinal cord by neuroprotective factors for motor neurons. J Neurosci Res 93:1184–1191

Tanimura A, Pancani T, Lim SAO, Tubert C, Melendez AE, Shen W, Surmeier DJ (2018) Striatal cholinergic interneurons and Parkinson's disease. Eur J Neurosci 47:1148–1158

Tanimura A, Du Y, Kondapalli J, Wokosin DL, Surmeier DJ (2019) Cholinergic interneurons amplify thalamostriatal excitation of striatal indirect pathway neurons in Parkinson's disease models. Neuron 101(444–458):e446

Tepper JM, Bolam JP (2004) Functional diversity and specificity of neostriatal interneurons. Curr Opin Neurobiol 14:685–692

Truong L, Brooks D, Amaral F, Henderson JM, Halliday GM (2009) Relative preservation of thalamic centromedian nucleus in parkinsonian patients with dystonia. Mov Disord 24:2128–2135

Villalba RM, Smith Y (2010) Striatal spine plasticity in Parkinson's disease. Front Neuroanat 4:133

Villalba RM, Smith Y (2011) Differential structural plasticity of corticostriatal and thalamostriatal axo-spinous synapses in MPTP-treated Parkinsonian monkeys. J Comp Neurol 519:989–1005

Villalba RM, Smith Y (2013) Differential striatal spine pathology in Parkinson's disease and cocaine addiction: a key role of dopamine? Neuroscience 251:2–20

Villalba RM, Smith Y (2017) Significant increase in the density of striatal cholinergic interneurons in the caudate nucleus of MPTP-treated parkinsonian monkeys. Soc Neurosc (Abstract) 757:13

Villalba RM, Smith Y (2018) Loss and remodeling of striatal dendritic spines in Parkinson's disease: from homeostasis to maladaptive plasticity? J Neural Transm (Vienna) 125:431–447

Villalba RM, Wichmann T, Smith Y (2014) Neuronal loss in the caudal intralaminar thalamic nuclei in a primate model of Parkinson's disease. Brain Struct Funct 219:381–394

Villalba RM, Mathai A, Smith Y (2015a) Morphological changes of glutamatergic synapses in animal models of Parkinson's disease. Front Neuroanat 9:117

Villalba RM, Lee S, Pare J-F, Smith Y (2015b) Glutamatergic denervation of striatal cholinergic interneurons in MPTP-treated parkinsonian monkeys. Soc Neurosc (Abstract) 217:05

Villalba RM, Pare J-F, Smith Y (2016) Three-dimensional electron microscopy imaging of spines in non-human primates. In: Bocstale EJV (ed) Transmission electron microscopy methods for understanding the brain. Springer Science + Business Media, New York, pp 81–103

Villalba RM, Pare J-F, Smith Y (2018) Differential ultrastructural reorganization of thalamo-cortical and cortico-cortical glutamatergic innervation in the primary motor cortex. Soc Neurosci (Abstract) 655:25

Wall NR, Wickersham IR, Cetin A, De La Parra M, Callaway EM (2010) Monosynaptic circuit tracing in vivo through Cre-dependent targeting and complementation of modified rabies virus. Proc Natl Acad Sci USA 107:21848–21853

Watanabe Y, Himeda T, Araki T (2005) Mechanisms of MPTP toxicity and their implications for therapy of Parkinson's disease. Med Sci Monit 11:RA17–RA23

West MJ (1999) Stereological methods for estimating the total number of neurons and synapses: issues of precision and bias. Trends Neurosci 22:51–61

Wickens JR, Arbuthnott GW, Shindou T (2007) Simulation of GABA function in the basal ganglia: computational models of GABAergic mechanisms in basal ganglia function. Prog Brain Res 160:313–329

Wolff M, Vann SD (2019) The cognitive thalamus as a gateway to mental representations. J Neurosci 39:3–14

Won L, Ding Y, Singh P, Kang UJ (2014) Striatal cholinergic cell ablation attenuates L-DOPA induced dyskinesia in Parkinsonian mice. J Neurosci 34:3090–3094

Yalcin-Cakmakli G, Rose SJ, Villalba RM, Williams L, Jinnah HA, Hess EJ, Smith Y (2018) Striatal cholinergic interneurons in a knock-in mouse model of L-DOPA-Responsive Dystonia. Front Syst Neurosci. 12, Article 28. https://doi.org/10.3389/fnsys.2018.00028 (eCollection 2018)

Yamanaka K, Hori Y, Minamimoto T, Yamada H, Matsumoto N, Enomoto K, Aosaki T, Graybiel AM, Kimura M (2018) Roles of centromedian parafascicular nuclei of thalamus and cholinergic interneurons in the dorsal striatum in associative learning of environmental events. J Neural Transm (Vienna) 125:501–513

Yelnik J, Percheron G, Francois C, Garnier A (1993) Cholinergic neurons of the rat and primate striatum are morphologically different. Prog Brain Res 99:25–34

Yuan HH, Chen RJ, Zhu YH, Peng CL, Zhu XR (2013) The neuroprotective effect of overexpression of calbindin-D(28k) in an animal model of Parkinson's disease. Mol Neurobiol 47:117–122

Zhai S, Tanimura A, Graves SM, Shen W, Surmeier DJ (2018) Striatal synapses, circuits, and Parkinson's disease. Curr Opin Neurobiol 48:9–16

Zhang D, Bordia T, McGregor M, McIntosh JM, Decker MW, Quik M (2014) ABT-089 and ABT-894 reduce levodopa-induced dyskinesias in a monkey model of Parkinson's disease. Mov Disord 29:508–517

Zheng X, Huang Z, Zhu Y, Liu B, Chen Z, Chen T, Jia L, Li Y, Lei W (2019) Increase in glutamatergic terminals in the striatum following dopamine depletion in a rat model of Parkinson's disease. Neurochem Res 44:1079–1089